

Improvement of alkali corrosion resistance of mullite ceramics at high temperature by depositing $\text{Ca}_{0.3}\text{Mg}_{0.2}\text{Zr}_2(\text{PO}_4)_3$ coating

Xiaozhen Zhang · Jianer Zhou · Jiandong Wang ·
Yuahua Jiang

Received: 26 November 2008 / Accepted: 6 March 2009 / Published online: 31 March 2009
© Springer Science+Business Media, LLC 2009

Abstract $\text{Ca}_{0.3}\text{Mg}_{0.2}\text{Zr}_2(\text{PO}_4)_3$ coating was deposited on the mullite ceramic to improve its alkali corrosion resistance at high temperatures, using sol–gel method and dip-coating technique. The phase composition and microstructure of the coating were characterized by X-ray diffraction and scanning electron microscopy (SEM). Results show that homogeneous, dense and single-phase $\text{Ca}_{0.3}\text{Mg}_{0.2}\text{Zr}_2(\text{PO}_4)_3$ coating was successfully deposited on mullite ceramics. SEM microstructural examination revealed the excellent bonding between $\text{Ca}_{0.3}\text{Mg}_{0.2}\text{Zr}_2(\text{PO}_4)_3$ coating and mullite ceramics. The effectiveness of the prepared coating to improve the alkali corrosion resistance of mullite ceramics was assessed through the measurements of mass loss and flexural strength degradation after 96 h and longer exposure time at alkali corrosion condition at 1000 °C. A significant enhancement of the alkali corrosion resistance for $\text{Ca}_{0.3}\text{Mg}_{0.2}\text{Zr}_2(\text{PO}_4)_3$ -coated mullite samples was observed. Therefore, the effectiveness of the $\text{Ca}_{0.3}\text{Mg}_{0.2}\text{Zr}_2(\text{PO}_4)_3$ material as protection coating for mullite ceramic is confirmed.

Introduction

Ceramics are well known for their thermal stability, and excellent resistance to wear and corrosion. Particularly challenging to the reliability of structural ceramic

components are those applications requiring good resistance to alkali attack at high temperatures [1, 2]. These applications include: refractories subjected to the action of alkali vapors in glass furnaces, cement kiln linings, combustion chamber boilers; and advanced high temperature coal conversion and combustion filters, heat exchangers, and other energy systems [3–6]. It has been found that many ceramics, such as Al_2O_3 , SiC, mullite, cordierite, and so on, would be attacked rapidly by alkali substances in these high-temperature applications [7–12]. Therefore, the protection of ceramics from alkali corrosion at high temperatures is urgently needed. There are many research efforts focused on corrosion prevention of Si-based ceramics, such as SiC and Si_3N_4 , used at high temperatures, using oxides or their composites as coating materials [13–15]. The application of these corrosion resistant materials as coatings on Si-based ceramic substrates, possessing the required mechanical properties for some specific applications, was confirmed to be a cost-effective way for optimizing both corrosion resistance and strength of the ceramic systems [14, 15].

Among the candidate materials for high-temperature applications, mullite ($\text{Al}_6\text{Si}_2\text{O}_{13}$) ceramics are considered to be one of the best materials, mainly because of its favorable properties, such as high thermal stability, low thermal expansion and conductivity, high creep resistance and corrosion stability together with suitable strength and fracture toughness [16]. Unfortunately, severe corrosion of mullite ceramics by various Na-salts was found to take place at temperatures up to 1000 °C [11, 12]. However, to the best of our knowledge, there are few published studies on corrosion prevention of mullite ceramics at high temperature. As a consequence, it is still a challenging task to improve the alkali corrosion resistance of mullite ceramics at elevated temperature.

X. Zhang (✉) · J. Zhou · J. Wang · Y. Jiang
National Research Center for Ceramic Engineering and
Technology, School of Material Science and Engineering,
Jingdezhen Ceramic Institute (JCI), Jingdezhen 333001,
Jiangxi Province, People's Republic of China
e-mail: zhangxz05@126.com

$\text{Ca}_{0.3}\text{Mg}_{0.2}\text{Zr}_2(\text{PO}_4)_3$ is a high-temperature thermal barrier material, which has the same crystal structure as $\text{NaZr}_2(\text{PO}_4)_3$ and shows low bulk thermal expansion, low crystal anisotropy, excellent thermal stability, and thermal shock resistance [17, 18]. An outstanding advantage for $\text{Ca}_{0.3}\text{Mg}_{0.2}\text{Zr}_2(\text{PO}_4)_3$ material to be used as coating on the mullite ceramics is that its coefficient of thermal expansion ($0.1\text{--}1.0 \times 10^{-6}/^\circ\text{C}$ at $25\text{--}1000^\circ\text{C}$) would match that of the mullite (ca. $4.0 \times 10^{-6}/^\circ\text{C}$ at $25\text{--}1000^\circ\text{C}$), which would yield an excellent thermal shock resistance of the coating [19]. However, the effectiveness for the $\text{Ca}_{0.3}\text{Mg}_{0.2}\text{Zr}_2(\text{PO}_4)_3$ coating to improve the alkali corrosion resistance of the mullite ceramics at elevated temperatures is still unknown and deserves to be investigated.

The sol–gel method is one of the most important techniques for preparing corrosion and oxidation-resistant ceramic coatings since it provides a high-purity, low-temperature synthesis and, especially, precise composition control [9, 20]. At the same time, the sol–gel method can overcome many disadvantages of conventional techniques because it is simple, less expensive, and allows coating on the component with complex geometry [9]. Consequently, this study focuses on the preparation of the $\text{Ca}_{0.3}\text{Mg}_{0.2}\text{Zr}_2(\text{PO}_4)_3$ coating on mullite ceramics by sol–gel method, and on the evaluation of the effectiveness for the $\text{Ca}_{0.3}\text{Mg}_{0.2}\text{Zr}_2(\text{PO}_4)_3$ coating to improve its alkali corrosion resistance under alkali corrosion conditions at 1000°C .

Experimental procedure

Preparation and surface pre-treatment of mullite substrate

The mullite ceramic samples in rectangular bar ($5\text{ mm} \times 6\text{ mm} \times 45\text{ mm}$) were prepared by mold pressing at 200 MPa , using commercially available mullite powder with a size range of 0.1 to $5.0\text{ }\mu\text{m}$ as main raw material, as well as $1.5\text{ wt}\%$ MgO as a sintering agent. The sintering of the mullite ceramics was conducted at 1550°C for 2 h .

In order to improve the adhesion of the coating, mullite samples were pretreated to remove possible contaminants on the substrate surface. Firstly, the samples were soaked in an ultrasonic cleaner containing acetone for 10 min , dried at 110°C for 2 h , and then immersed in a solution containing $5\text{ wt}\%$ HF for 5 min . Finally, samples were washed with deionized water and dried at 120°C for 2 h .

Preparation of sol-gel solution

The reagents selected for the sol–gel solution were calcium nitrate ($\text{Ca}(\text{NO}_3)_2 \cdot 4\text{H}_2\text{O}$), magnesium nitrate ($\text{Mg}(\text{NO}_3)_2 \cdot 6\text{H}_2\text{O}$), zirconium oxychloride ($\text{ZrOCl}_2 \cdot 8\text{H}_2\text{O}$), and triethyl phosphate ($(\text{C}_2\text{H}_5\text{O})_3\text{P}(\text{O})$). The reagents were mixed

in stoichiometric ratio, based on the formula of $\text{Ca}_{0.3}\text{Mg}_{0.2}\text{Zr}_2(\text{PO}_4)_3$, in absolute ethyl alcohol. The mixture was constantly stirred while ammonia water was added dropwise until a pH value between 2.0 and 4.0 was reached. Sol solutions with $\text{Ca}_{0.3}\text{Mg}_{0.2}\text{Zr}_2(\text{PO}_4)_3$ concentrations at $10\text{--}35\text{ wt}\%$ could be obtained by controlling the amount of ethyl alcohol.

Elaboration of $\text{C}_{0.6}\text{M}_{0.4}\text{ZP}$ coating

$\text{Ca}_{0.3}\text{Mg}_{0.2}\text{Zr}_2(\text{PO}_4)_3$ coating was deposited on the mullite ceramic by dip-coating techniques. First, surface-pretreated mullite samples were soaked in the $\text{Ca}_{0.3}\text{Mg}_{0.2}\text{Zr}_2(\text{PO}_4)_3$ sol for 5 min and withdrawn at a lift rate of 8 cm/min . The coated samples were then dried at 25°C and 55% relative humidity for 48 h , and at 60°C for another 24 h . Finally, the coated samples were thermally processed at 1350°C for 2 h to remove residual solvent, organic components, and crystallize the amorphous gel to form dense coating. The formation of crack was avoided by using a step heating schedule. The samples were successively heated up to 200°C at a rate of 0.5°C/min and 500°C with 1.0°C/min and remained at each step for 1 h . They were then heated up at a rate of 5°C/min to 1000°C for 1 h and sintered at 1350°C for 3 h .

For multiple coating depositions, successive coatings were applied after the pre-coated sample was thermally processed at 500°C for 1 h . The sample was heated up to 500°C with the same heating procedure as described above.

Characterization methods

Phase compositions were identified by X-ray diffraction (XRD, D8 Advance, Bruker, Germany) with $\text{Cu K}\alpha$ radiation ($\lambda = 0.154\text{ nm}$), working voltage 40 kV , working current 50 mA , and scanning speed of $0.02^\circ/\text{s}$. Thermogravimetric analysis (TGA) and differential scanning calorimetry (DSC) (TGA-DSC, STA449C, Netzsch, Germany) were carried out from ambient temperature to 1100°C at a heating rate of 10°C/min under air. Contact angle analyzer (VCA Optima/VCA 3000S, AST, USA) was used to determine the wetting angle of mullite samples, using deionized water drop.

Microstructure of the sintered porous-supported samples was observed using scanning electron microscopy (SEM, JEOM, JSM-6700F, Japan). The elemental distribution in the samples was measured by Philips EDAX energy dispersive spectroscopy (EDS) attached to the SEM. The bending strength was determined by the three-point bending method using a universal testing machine (Instron 5566, Instron, USA), with a crosshead speed of 0.25 mm/s and span length of 30 mm .

The alkali corrosion resistance of both coated and uncoated mullite ceramics was determined by measuring

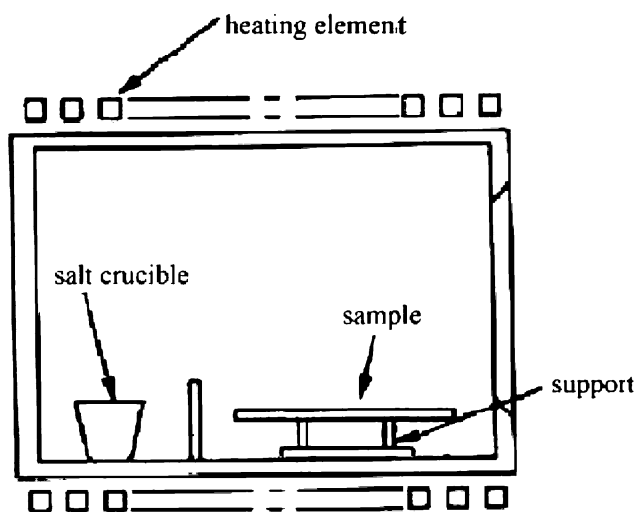


Fig. 1 Schematic of apparatus used for the alkali corrosion test

the mass loss and flexural strength degradation of samples exposed to Na-salt atmosphere at 1000 °C for 48 h. Na_2CO_3 was selected as the alkali source, to simulate the coal combustion conditions in real industrial systems. Weighed samples were first heated to 250 °C and then dipped into a saturated Na_2CO_3 aqueous solution to deposit a Na_2CO_3 film. The amount of the salt adhering to the surface of samples was calculated to be 4.2 mg/cm². The samples were then put in a furnace and exposed to an atmosphere containing Na-salts at 1000 °C for 48 h. An alumina crucible filled with sufficient Na_2CO_3 was also placed in the furnace. By measuring the mass loss of Na_2CO_3 and assuming that the vapor behaves as an ideal gas at high temperatures, the concentration of Na-salt was calculated to be about 5.6 vol.%. To investigate the mass loss and strength degradation as a function of time, corrosion experiment at 1000 °C for 360 h was also conducted. The schematic of the apparatus used for the alkali corrosion tests is illustrated in Fig. 1.

In order to get the mass loss after alkali corrosion, the samples were first washed in distilled water at 100 °C to remove water soluble phases such as residual salts and sodium silicates, and then etched in 10% HCl solution to remove the surface corrosion product layer. Prior to weighing, the samples were dried in an oven at 120 °C for 2 h. This entire procedure was repeated until no mass change was observed.

Results and discussion

Influence of surface pre-treatment on contact angle

Contact angle tests were conducted to evaluate the effectiveness of the surface pre-treatment. Four measurements

were performed on each sample to get an average value. It is found that the contact angle for untreated and pretreated mullite samples is 57.2 and 32.8°, respectively. Good wetting of the substrate surface and spreading of the water drops was observed for the pretreated samples as indicated by the smaller contact angle. A significant decrease in contact angle after treatment suggests that the adhesion of the coating to the surface of mullite substrate is enhanced.

Characterization of sol-gel-derived $\text{C}_{0.6}\text{M}_{0.4}\text{ZP}$ precursor

Figure 2 shows the TGA-DTA curves for the sol-gel-derived $\text{Ca}_{0.3}\text{Mg}_{0.2}\text{Zr}_2(\text{PO}_4)_3$ precursor. The TGA curve indicates an overall mass loss of about 41% and much of the loss takes place below 400 °C. The DTA curve shows two obvious endothermic peaks at about 90 and 230 °C, respectively. Accordingly, there are two mass loss stages at different temperature ranges in TGA curve. The endothermic peak at 90 °C is due to the removal of absorbed water, and the endothermic peak at 230 °C can be attributed to the elimination of NO_3^- ions, crystal water, and organic substances. The exothermic peak at about 830 °C can be related to the crystallization of $\text{Ca}_{0.3}\text{Mg}_{0.2}\text{Zr}_2(\text{PO}_4)_3$ powder, as confirmed by the XRD patterns in Fig. 3.

XRD was used to further investigate whether the sol-gel procedure successfully synthesized the desired compounds. The XRD patterns of $\text{Ca}_{0.3}\text{Mg}_{0.2}\text{Zr}_2(\text{PO}_4)_3$ gels calcined at different temperatures for 3 h are shown in Fig. 3. After heating up to 750 °C, the gel showed the presence of $\text{Ca}_{0.3}\text{Mg}_{0.2}\text{Zr}_2(\text{PO}_4)_3$ phase, but mainly in amorphous form. The XRD pattern of samples calcined at 1200 °C for 3 h showed sharp peaks, indicating a pure and well-crystallized $\text{Ca}_{0.3}\text{Mg}_{0.2}\text{Zr}_2(\text{PO}_4)_3$ phase.

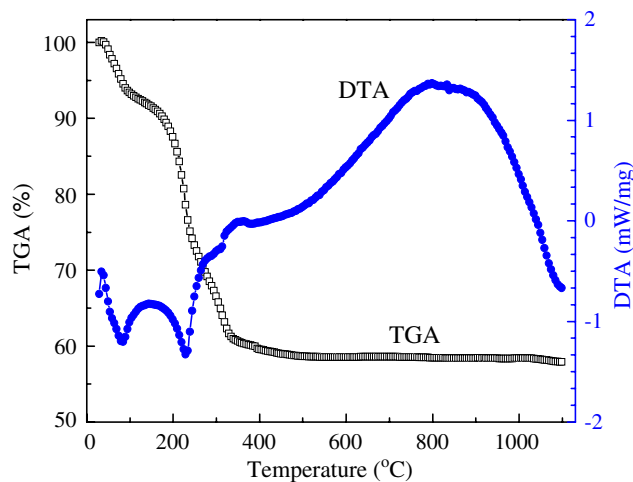


Fig. 2 TGA-DTA curves of $\text{Ca}_{0.3}\text{Mg}_{0.2}\text{Zr}_2(\text{PO}_4)_3$ dry gel

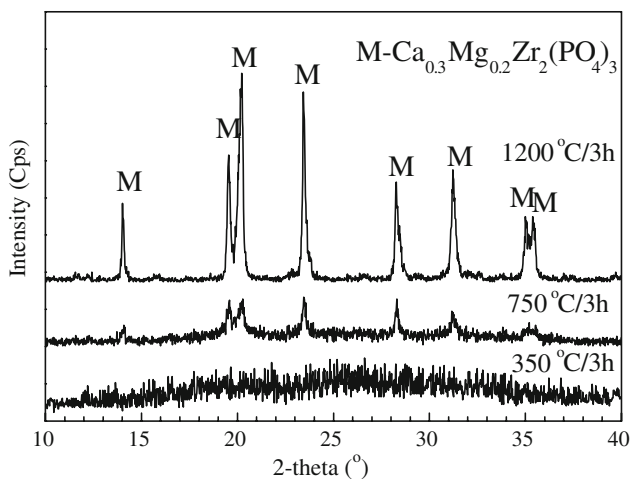


Fig. 3 XRD patterns of $\text{Ca}_{0.3}\text{Mg}_{0.2}\text{Zr}_2(\text{PO}_4)_3$ dry gel calcined at different temperatures for 3 h

Microstructure of $\text{C}_{0.6}\text{M}_{0.4}\text{ZP}$ coating

The $\text{Ca}_{0.3}\text{Mg}_{0.2}\text{Zr}_2(\text{PO}_4)_3$ coating was deposited on the mullite ceramic substrates, using the sol–gel and dip-coating techniques. Figure 4 shows the microstructure of the surface and the cross section of the coated sample derived from sol with a concentration of 25 wt%, pH = 3.2, and with two dipping cycles. As observed in Fig. 4a, the coating on the mullite ceramic is uniformly distributed and composed of near equiaxed grains with a diameter of 1 to 3 μm . Moreover, the prepared coating is well adhered to the mullite substrate after sintered at 1350 °C for 3 h, as illustrated in Fig. 4b. The thickness of the prepared $\text{Ca}_{0.3}\text{Mg}_{0.2}\text{Zr}_2(\text{PO}_4)_3$ coating is about 3.0 μm (Fig. 4b). SEM observations revealed that the formation of crack-free, smooth, and intact coating was strongly dependent on the sol concentration, pH, viscosity, and dipping times. A sol concentration between 25 and 30 wt% and dipping for two to three cycles is necessary to avoid poor coverage of the surface and spalling of the coating. The thickness of the $\text{Ca}_{0.3}\text{Mg}_{0.2}\text{Zr}_2(\text{PO}_4)_3$ coating was

found to be varied between 1.5 and 5.0 μm , mostly depending on the selected sol viscosity and dipping times. However, with only once dipping, the prepared coating cannot completely cover the mullite substrate, even though using a sol concentration of 30 wt%.

Evaluation of alkali corrosion resistance

The mullite ceramic samples coated for two cycles with 25 wt% $\text{Ca}_{0.3}\text{Mg}_{0.2}\text{Zr}_2(\text{PO}_4)_3$ sol as well as those uncoated samples were tested in Na-salt atmosphere at 1000 °C for 48 h. Table 1 lists the mass loss and flexural strength degradation after corrosion tests. As can be seen, the uncoated samples exhibited a much greater mass loss (2.18%) after alkali attack than that of coated samples (0.27%). Strength degradation of mullite ceramics in harsh environments is of prime concern because it can set serious limitation to their use in structural applications. As listed in Table 1, the strength of all the samples was found to decrease below their initial values after corrosion. The flexural strength significantly decreased by 53.1% for uncoated samples, whereas only 5.7% for $\text{Ca}_{0.3}\text{Mg}_{0.2}\text{Zr}_2(\text{PO}_4)_3$ coated samples. It must be mentioned that the application of $\text{Ca}_{0.3}\text{Mg}_{0.2}\text{Zr}_2(\text{PO}_4)_3$ coating did not significantly affect the initial strength of mullite ceramics. Therefore, the alkali corrosion resistance of $\text{Ca}_{0.3}\text{Mg}_{0.2}\text{Zr}_2(\text{PO}_4)_3$ -coated mullite is obviously improved over that of uncoated ceramics. This can also be confirmed by the SEM observation shown in Fig. 5. As seen, the surface of the mullite sample is very smooth and dense before corrosion test (Fig. 5a). However,

Table 1 Mass loss and strength change of $\text{Ca}_{0.3}\text{Mg}_{0.2}\text{Zr}_2(\text{PO}_4)_3$ coated and uncoated samples after alkali corrosion

Samples	Mass loss after corrosion (%)	Strength (MPa)	
		Before corrosion	After corrosion
Uncoated	2.18	131.6	61.7
Coated	0.27	132.8	125.2

Fig. 4 a Surface and b cross-sectional SEM micrographs of the mullite sample coated with $\text{Ca}_{0.3}\text{Mg}_{0.2}\text{Zr}_2(\text{PO}_4)_3$ coating

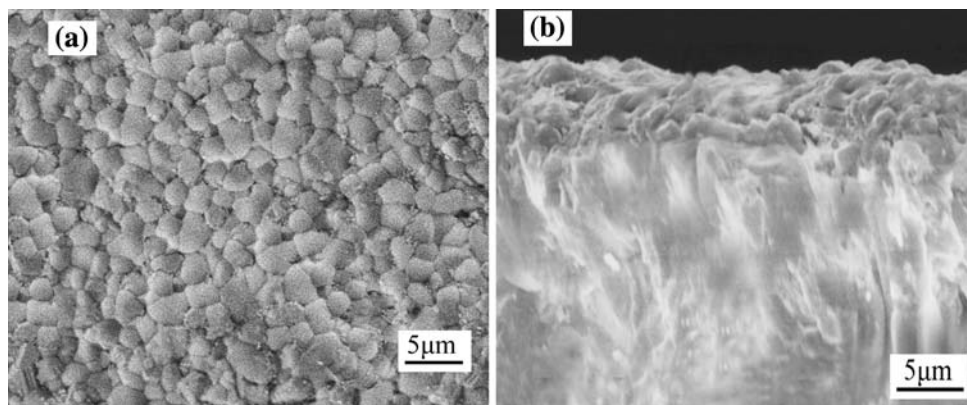
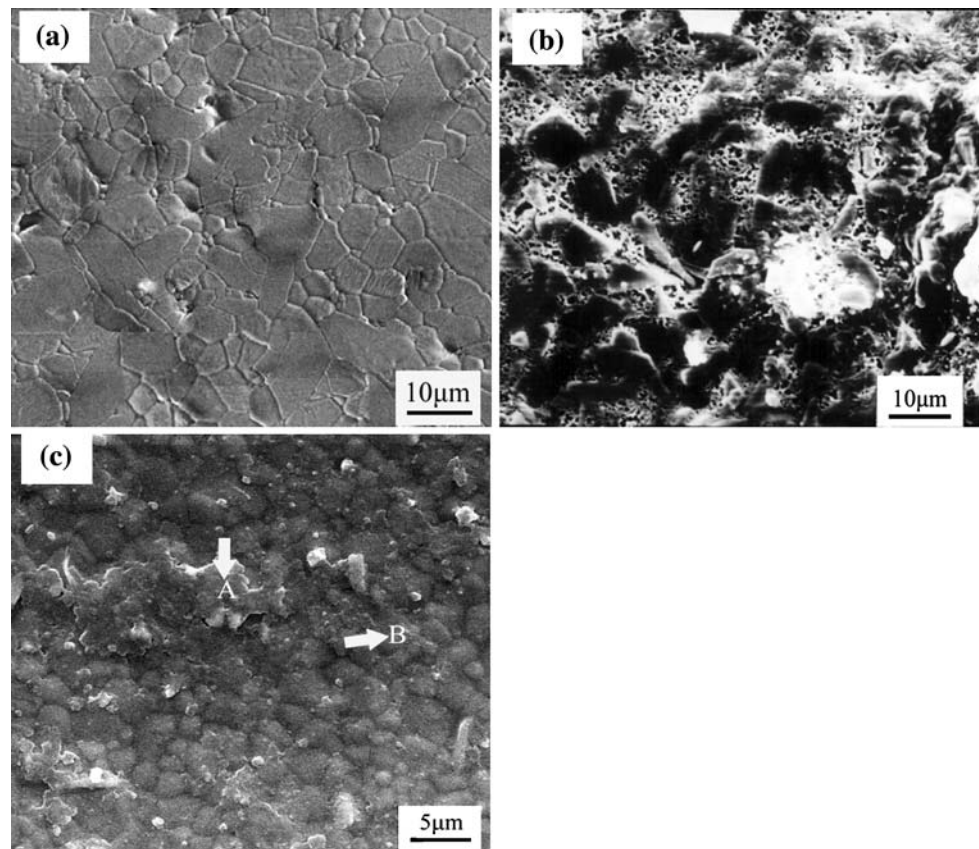


Fig. 5 SEM micrographs of **a** as-received mullite ceramic, **b** mullite ceramic, and **c** coated mullite ceramic after corrosion



lots of small reticular pores, and even small cracks were formed on the surface of the uncoated sample, after being subjected to Na-salt atmosphere at 1000 °C for 48 h (Fig. 5b). This suggests that the uncoated sample was severely corroded. As observed in Fig. 5c, the $\text{Ca}_{0.3}\text{Mg}_{0.2}\text{Zr}_2(\text{PO}_4)_3$ coating on the mullite sample is still intact after alkali attack, and no obvious destruction to the coated sample is observed. These SEM observations are in accordance with the mass loss and strength degradation results (Table 1). It also must be noted some separated and irregular flakes, e.g., spot A in Fig. 5c, are observed on the local surface of coated samples after the corrosion test.

EDS analysis was conducted to determine the composition of the surface for coated sample after corrosion test. The EDS spectra, corresponding to spots A and B in Fig. 5c,

were shown in Fig. 6a, b, respectively. As observed in Fig. 6b, the detected elements on the coating particle (spot B in Fig. 5c) are mainly Zr, P, Mg, Ca, Al, Si, and O, which are from the coating material and mullite substrate, and only traces of Na is observed. This suggests that no significant corrosion attack of the $\text{Ca}_{0.3}\text{Mg}_{0.2}\text{Zr}_2(\text{PO}_4)_3$ coating occurs in the Na-salt containing environment at 1000 °C for 48 h. Nevertheless, Fig. 6a shows that peak intensity of Na in the irregular flake deposit (spot A in Fig. 5c) is much higher than that of the particles (spot B in Fig. 5c). Combined with the result shown in Figs. 6 and 5c, it can be deduced that irregular flakes are mainly derived from the deposition of Na-salt during cooling, since the alkali corrosion test was conducted in a relatively closed environment with enough Na_2CO_3 as alkali source. The irregular deposits are

Fig. 6 EDS spectra of coated samples after alkali corrosion corresponding to **a** spot A and **b** spot B in Fig. 5c

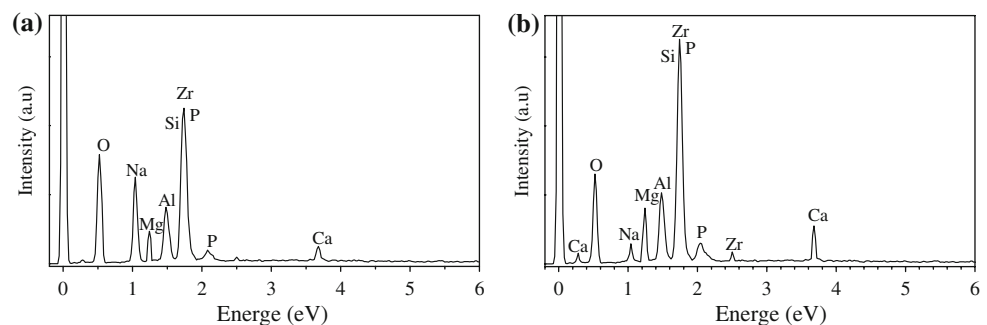
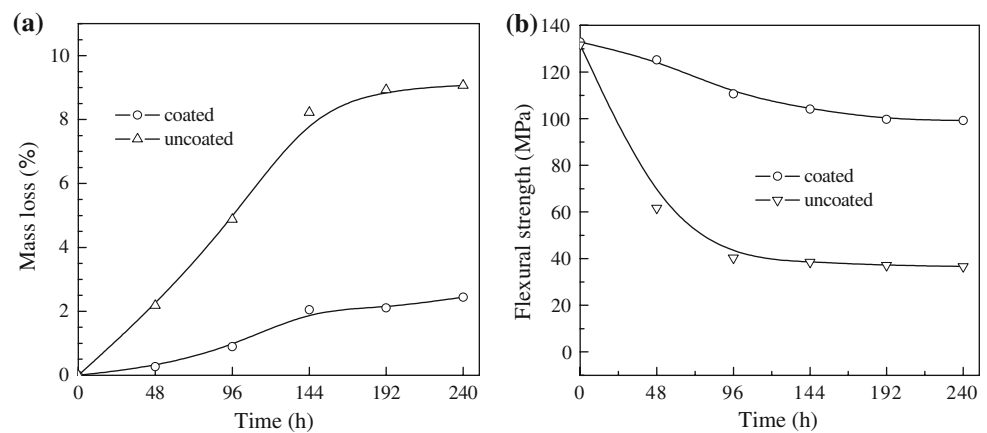


Fig. 7 Mass loss and flexural strength as a function of time after alkali corrosion



probably composed of fine Na-salt particles, and the Na-salt shows no obvious corrosion attack on the coated samples.

The mass loss and flexural strength measurements as a function of time were also investigated and are shown in Fig. 7. The weight loss is 9.07 and 2.44% and the flexural strength reduction after 240 h corrosion is 72.6 and 25.3% of the initial strength for uncoated and $\text{Ca}_{0.3}\text{Mg}_{0.2}\text{Zr}_2(\text{PO}_4)_3$ -coated samples, respectively. So, the $\text{Ca}_{0.3}\text{Mg}_{0.2}\text{Zr}_2(\text{PO}_4)_3$ coating is proved to be effective in enhancing the alkali corrosion resistance of mullite ceramics at 1000 °C, even undergoing long-time aging.

It can be observed in Fig. 7a that mass loss measurements for uncoated samples indicate a two-step kinetic process for the corrosion reaction, regardless of the coatings. A rapid consumption of the mullite ceramic is evidenced by a substantial increase in the weight loss over the first 144 h testing. This stage is probably associated with the dissolution of mullite and the formation of a liquid melt through which sodium vapor diffuses and readily corroded mullite. Then, the weight loss curves reach a plateau, indicating a slowing corrosion.

The strength degradation can be attributed to the propagation of crack originating from the reticular pores. This mechanism of failure is well known and is explained in terms of stress concentration around the pore-like defects. According to the relationship between strength and porosity proposed by Duckworth [21], the strength degradation is directly correlated to the pore size and content. Based on the equation of Duckworth, the higher fracture strength yielded by mullite ceramics coated with $\text{Ca}_{0.3}\text{Mg}_{0.2}\text{Zr}_2(\text{PO}_4)_3$ can be attributed to fewer pores in the ceramic body after alkali attack.

Conclusions

Single-phase $\text{Ca}_{0.3}\text{Mg}_{0.2}\text{Zr}_2(\text{PO}_4)_3$ coating on mullite ceramics was prepared successfully using sol-gel method

and dip-coating techniques. Homogeneously, dense $\text{C}_{0.6}\text{M}_{0.4}\text{ZP}$ coating and a good coverage of coating to the mullite ceramics were achieved using a solution concentration of 25 wt% $\text{Ca}_{0.3}\text{Mg}_{0.2}\text{Zr}_2(\text{PO}_4)_3$ precursor and a lift rate of 8 cm/min. The prepared coating shows a thickness of about 3.0 μm after two dipping cycles. The alkali corrosion resistance of mullite ceramics was greatly improved after coating with $\text{Ca}_{0.3}\text{Mg}_{0.2}\text{Zr}_2(\text{PO}_4)_3$. The weight loss and flexural strength degradation of coated mullite ceramics were much less than those of uncoated after Na-salt corrosion at 1000 °C for 48–240 h. Further study is being carried out on the optimization of processing conditions for the coating preparation as well as systematical investigation of the corrosion protection performance of $\text{Ca}_{0.3}\text{Mg}_{0.2}\text{Zr}_2(\text{PO}_4)_3$ -coated mullite ceramics in real industrial combustion environments above 1000 °C.

References

1. Akira O (2008) *J Eur Ceram Soc* 28:1097
2. Alvin MA (1996) *Ind Eng Chem Res* 35:3384
3. Lippert TE, Lane JE (1991) *Am Ceram Soc Bull* 70:1491
4. Fredericci C, Morelli MR (2000) *Mater Res Bull* 35:2503
5. Aksel C (2003) *Ceram Int* 29:305
6. Moya JS, Steier HP, Requena J (1999) *Composites Part A* 30:439
7. Fritsch M, Klemm H, Herrmann M, Schenk B (2006) *J Eur Ceram Soc* 26:3557
8. Hirata T, Ota S, Morimoto T (2003) *J Eur Ceram Soc* 23:91
9. Jacobson NS, Opila EJ, Lee KN (2001) *Curr Opin Solid State Mater Sci* 5:301
10. Takahashi J, Kawai Y, Shimada S (1998) *J Eur Ceram Soc* 18:1121
11. Takahashi J, Kawai Y, Shimada S (2002) *J Eur Ceram Soc* 22:1959
12. Jacobson NS, Lee KN, Yoshio T (1996) *J Am Ceram Soc* 79:2161
13. Ueno S, Jayaseelan DD, Ohji T (2004) *Int J Appl Ceram Technol* 1:362
14. Lee KN (2000) *Surf Coat Technol* 133–134:1
15. Lee KN, Miller RA (1996) *Surf Coat Technol* 86–87:142

16. Schneider H, Schreuer J, Hildmann B (2008) *J Eur Ceram Soc* 28:329
17. Li TK, Hirschfeld DA, Vanaken S (1993) *J Mater Res* 8:2954
18. Russ WM (1994) Master's Thesis, Department of Materials Science and Engineering, Virginia Tech
19. Breval E, Mckinstry HA, Agrawal DK (2000) *J Mater Sci* 35:3359. doi:[10.1023/A:1004828917908](https://doi.org/10.1023/A:1004828917908)
20. Jacques L (1997) *Curr Opin Solid State Mater Sci* 2:132
21. Duckworth W (1953) *J Am Ceram Soc* 36:68